Supporting Information

Understanding the Interaction of Block Copolymers with DMPC Lipid Bilayer using Coarse-Grained MD Simulations

Samira Hezaveh[a], Susruta Samanta, Antonio De Nicola[b,c], Giuseppe Milano[b,c] and Danilo Roccatano[a*]*

[a] Jacobs University Bremen, Campus Ring 1, D-28759 Bremen, Germany

[b] Dipartimento di Chimica e Biologia and NANOMATES, Research Centre for NANOMAterials and nanoTEchnology at Università di Salerno, I-84084 via Ponte don Melillo Fisciano (SA), Italy

[c]IMAST Scarl-Technological District in Polymer and Composite Engineering, P.le Fermi 1, 80055 Portici (NA), Italy

Contents:

1. CG force field parameterization.

The CG models for the PEO and PPO blocks were parameterized on atomistic models of the two polymers[1]. The MARTINI force field.[2,3] was used for bond, bond angles and Lennard-Jones (LJ) potential functions. The initial set of CG bonded parameters for PEO and PPO were obtained by fitting the bond and bond-angle distributions obtained from the atomistic simulations.[1] These parameters specifically were adjusted to get the best match between the distributions of atomistic PEO43 and PPO43 models and their CG ones.

In Figure 1S bond and angle distributions obtained from the mapping of the atomistic model to the CG one are shown. The angle distributions, $p(\theta)$, was weighted by a factor $sin\theta$ to take metric tensor effects into account,[4]

$$P(\theta) = f_n \frac{p(\theta)}{\sin\theta} \qquad (1)$$

where f_n is normalization factor.

First we started by fitting the atomistic distributions of these geometrical quantities with Gaussian functions. The position of the Gaussian peak was used for the reference bond-angle or bond distance in harmonic potential functions. As shown in the Figure 1S, atomistic bond distributions have single peak while in case of bond-angle distributions a second small peak or a shoulder is present on the left side of the main peak. Since this second peak does not give a large contribution to the total distributions, we decided to simplify the potentials by fitting both peaks with a single Gaussian distribution as shown with a solid lines in Figure 1S.

Figure 1S. Bond and bond-angle distribution curve obtained from atomistic and optimized MARTINI CG models for PEO and PPO. The solid lines are the Gaussian fits to atomistic distributions.

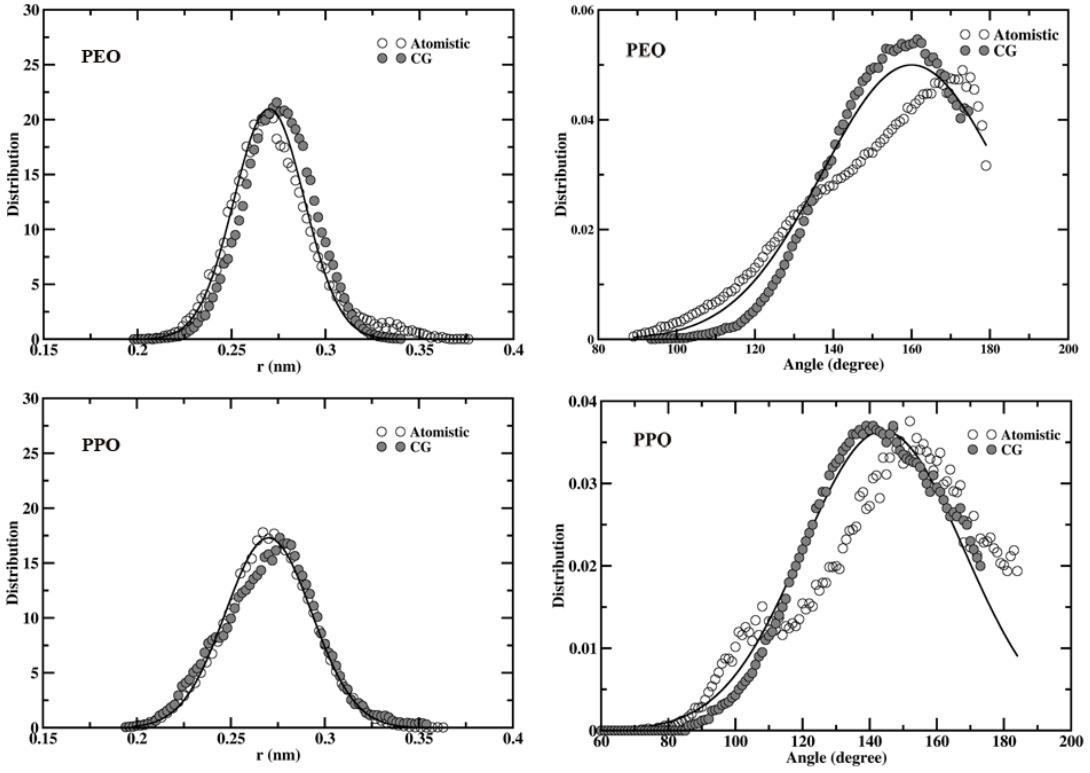

The values of the force constants obtained by using the spring constant equation, $4kT/\sigma^2$(σ is the width of fitted curve)[4] and they have been further adjusted for a better reproduction of the atomistic model properties. The final bond and bond-angle parameters for MARTINI CG model are reported in Table 1 of the paper.

In the case of non-bonded potential parameters, the first set of values was assigned from the Lennard-Jones (LJ) pair interaction library of MARTINI force-field. The values of σ parameters for PEO-PEO, PPO-PPO and PEO-PPO beads LJ interactions were further refined by calculating oxygen-oxygen radial distribution functions (RDF) for liquid dimethoxyethane

(DME) and dimethoxypropane (DMP)[1] respectively. RDFs of O_{DME}-O_{DME}, O_{DMP}-O_{DMP} and O_{DME}-O_{DMP} pairs at 298 K were calculated from atomistic simulations. For the first two RDFs (O_{DME}-O_{DME}, O_{DMP}-O_{DMP}) the calculations were performed using simulation boxes containing 216 molecules. RDF of O_{DME}-O_{DMP} was calculated in a system including one DME in 215 DMP, as shown in Figure 2S.

Figure 2S. RDFs of O_{DME}-O_{DME}, O_{DMP}-O_{DMP} and O_{DME}-O_{DMP} pairs at 298 K from atomistic simulations in their liquid phase of DME and DMP systems.

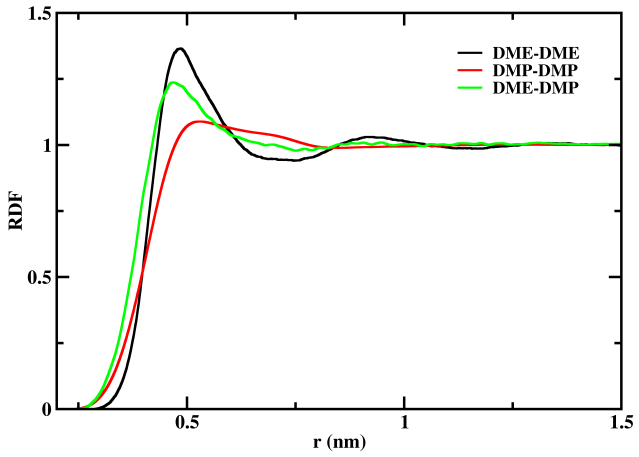

The values of σ parameter were taken as the positions of the first peak in the RDF and their final values reported in Table 1 of the manuscript.

The initial value the ε parameter for PEO-PEO interaction was taken from SP1 particle type with H-bonding acceptor properties (ε=3.375 kJ mol^{-1} and σ= 0.43 nm). The value was further refined by comparing the radii of gyration in water for different chain length obtained from the CG simulations with those from the corresponding atomistic simulations and the experimental extrapolated data.[1,6] The best agreement was provided by choosing a value of ε=3.5 kJ mol^{-1} with σ= 0.48 nm for PEO-PEO interaction.

[1] They can be considered the shortest oligomers of PEO and PPO[5].

The same procedure was used to obtain the ε parameter for the PPO-PPO interaction. The starting values for this interaction were SC3 (ε=2.6 kJ mol^{-1} with σ= 0.43 nm). Using this particle type resulted in a too small R_g values compared to the corresponding atomistic ones. Therefore we tried to adjust the interactions in order to get the closest values of R_g to the atomistic ones. Therefore, the σ value of PPO-PPO interaction parameter was modified to the optimal value of σ= 0.50 nm (from RDF calculations, see Figure 2S) and the value of the interaction with water (PPO-P4) also was set to ε=3.5 kJ mol^{-1} to get the CG R_g values closer to the atomistic ones. Finally, the value of the PEO-PPO interaction was set to ε=2.9 kJ mol^{-1} based on the comparison of the calculated R_g of P85 with the experimental one in water at 293 K. Final parameters are reported in Table 1 of the paper.

2. Simulations of PEO and PPO chains in water.

Single chains of PEO and PPO of lengths *n*= 9, 18, 27, 36, 43, 76, 135 and 159 were simulated in water at 298 K. The runs were performed for different simulation time accordingly to the chain length, *n*= 9, 18, 27 (~200-400 ns); 36, 43, 76, 135 and 159 (~500-900 ns) for PEO. Simulation boxes were ~7-12 nm/side depending on the length of polymer and contained ~3000-19000 water molecules.

In Figure 3S, the radii of gyration (values in Table 1S) were plotted vs. molecular weigths for all chains. The curves were fitted using the exponential law [6],

$$R_g = aM_W^{\nu} \qquad (2)$$

where M_w is the molecular weight and ν is the Flory exponent.[7] Fitting our R_g values to this equation, we obtained,

$$R_g = 0.021 \times M_W^{0.58} \quad (3)$$

Our result was compared with the available extrapolated experimental one[6] obtained from light scattering data of PEO from chain of molecular weight (ranging from ~10^4 to 10^7) which is,

$$R_g = 0.020 \times M_W^{0.58} \quad (4)$$

The comparison shows an excellent agreement with the one obtained from our CG model. Both experimental and simulated exponents are in good agreement with the Flory theory of a polymer chain in a good solvent (ν=0.6) and with more sophisticated group renormalization theories (ν=0.588). [7]

Since PPO is not soluble in water and there were no experimental values for comparison, thus the CG R_g values were compared only with those from atomistic simulations.[1] As shown in Figure 3S, the values of R_g are in good agreement with the atomistic ones (up to 43 units). However, longer PPO chains tend to be more compact than the corresponding PEO ones since the hydrophobicity increases with the chain length. The effect is more evident for the longer chains like the PPO159. At the end we fitted the R_g values of PPO using exponential law, Eq. 2. The power law turned out to be,

$$R_g = 0.138 \times M_W^{0.26} \quad (5)$$

The result shows that the ν value is comparable to the Flory power of polymer in a bad solvent, which is 1/3.

Table 1S. Average radii of gyration (in nm) for PEO and PPO chains at 298 K.

n	PEO	PPO
9	0.68±0.01	0.61±0.01
18	1.06±0.1	0.90±0.3
27	1.34±0.3	1.03±0.3

36	1.55±0.2	1.08±0.2
43	1.76±0.1	1.16±0.3
76	2.43±0.4	1.25±0.2
135	3.15±0.2	1.33±0.1
159	3.48±0.2	1.40±0.2

Figure 3S. Radius of gyration vs. molecular weight for PEO (top) and PPO (bottom) polymer chains. The experimental curve for PEO was extrapolated from the experimental data of polymer having higher molecular weight. For comparison, the values obtained from the atomistic model are also shown for both polymers.

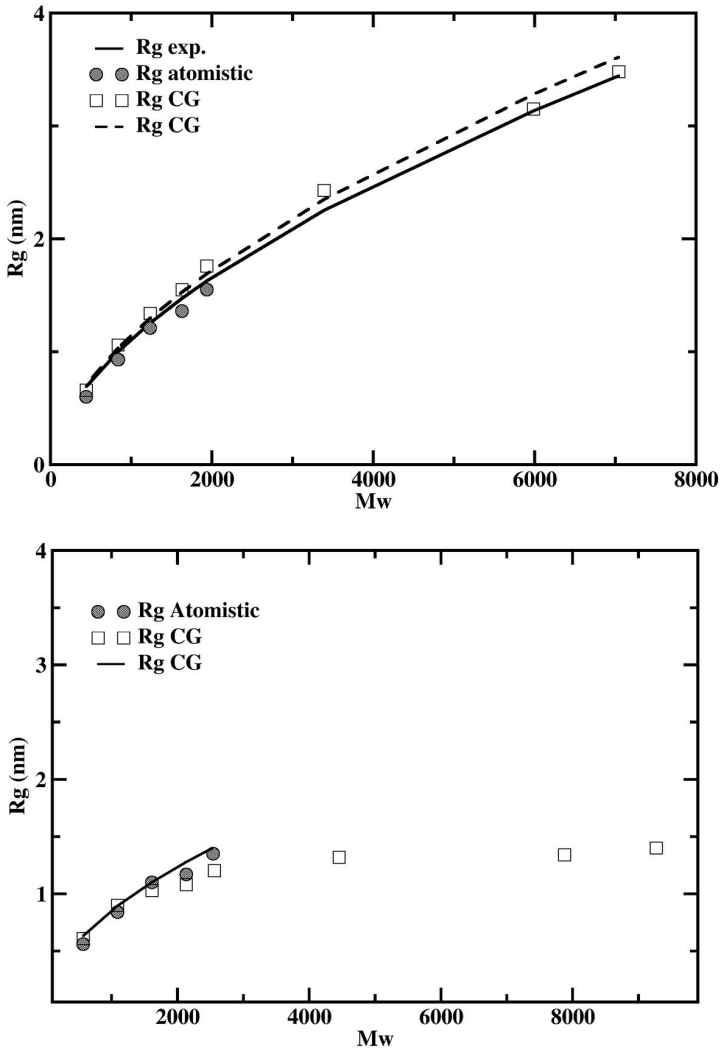

3. Potential of mean force for the permeation of CG DME and DMP in the DMPC lipid bilayer.

Umbrella sampling (US) method was used to calculate the CG free energy profiles for the percolation of the DME and DMP through upper layer of the DMPC bilayer. This method has been previously implemented and described in our previous work where we calculated the PMF profiles for DME and DMP for the atomistic model.[8] In the present work, we have adopted similar parameters. Initially a steered molecular dynamics (SMD) simulation was run to pull the DME/DMP molecules inside the DMPC bilayer. ~40 starting configurations were taken from the path of the SMD trajectory. A harmonic restraint with a force constant 3000 kJ/mol nm^2 was applied to the distance between the center of mass (CoM) of the DME/DMP molecule and the head groups of the bottom DMPC layer, in the direction normal to the bilayer. The first configurations were taken at least 3 nm away from the bilayer center and the last one in the bilayer center. The difference of distances between the CoM of the DME/DMP molecules and reference group for two consecutive conformations was always less than 0.1 nm to ensure the correct calculation of PMF profile. Each frame was simulated for 20 ns. The weighted histogram analysis method (WHAM)[9] was used to calculate the PMF profile. The free energy profiles obtained from the calculations were rescaled to assign a zero reference value to the profiles in the bulk water. In figure 4S, the calculated profile for DME and DMP compared with the atomistic curves are reported. For comparison all the curves have been shifted to zero value in the water phase.

Figure 4S. Comparison of PMF profiles DME and DMP (both atomistic and coarse-grained models) calculated using umbrella sampling method.

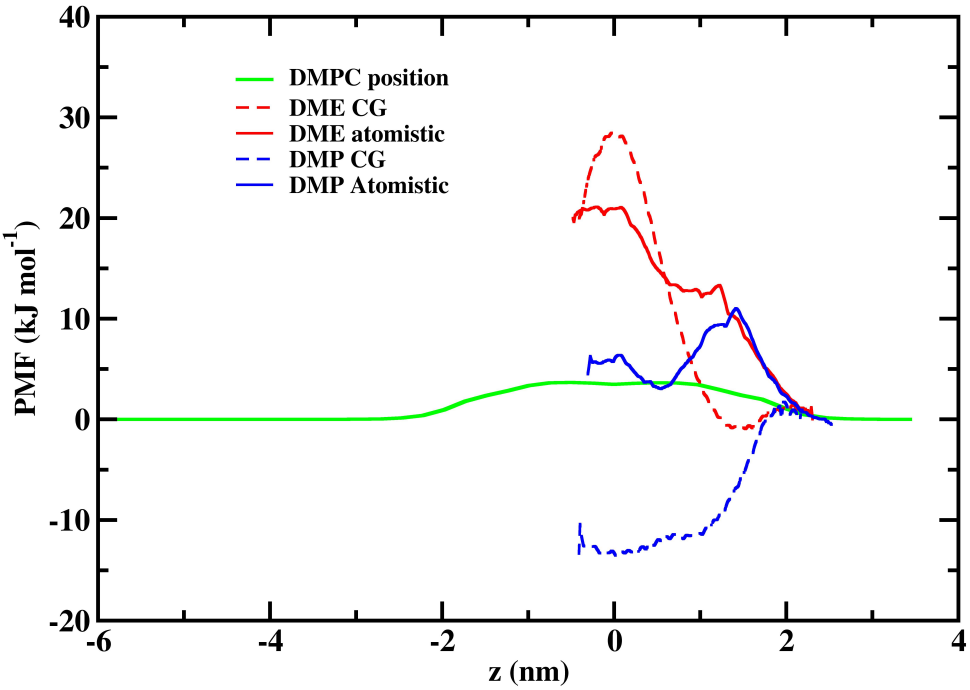

4. Area per lipid.

Figure 5S. Time series of the area per lipid for the different simulations presented in the paper.

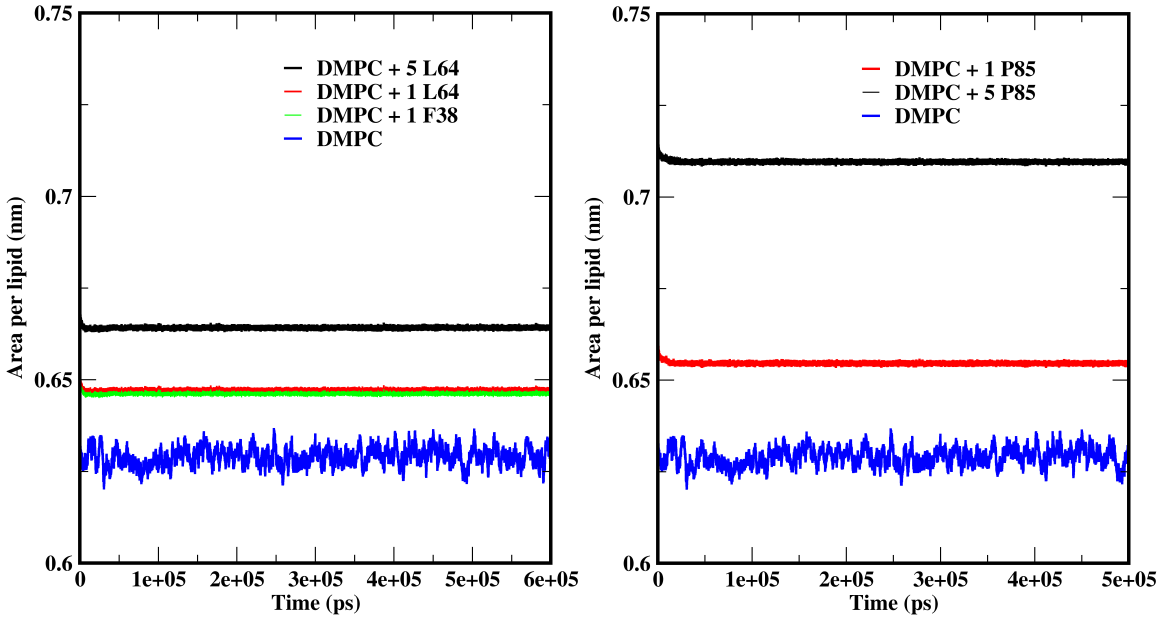

5. Interaction of Pluronics with DMPC bilayer.

Figure 6S. Snapshots from the simulation with L64 on top of the DMPC bilayer. The insertion of PPO block in the tail groups.

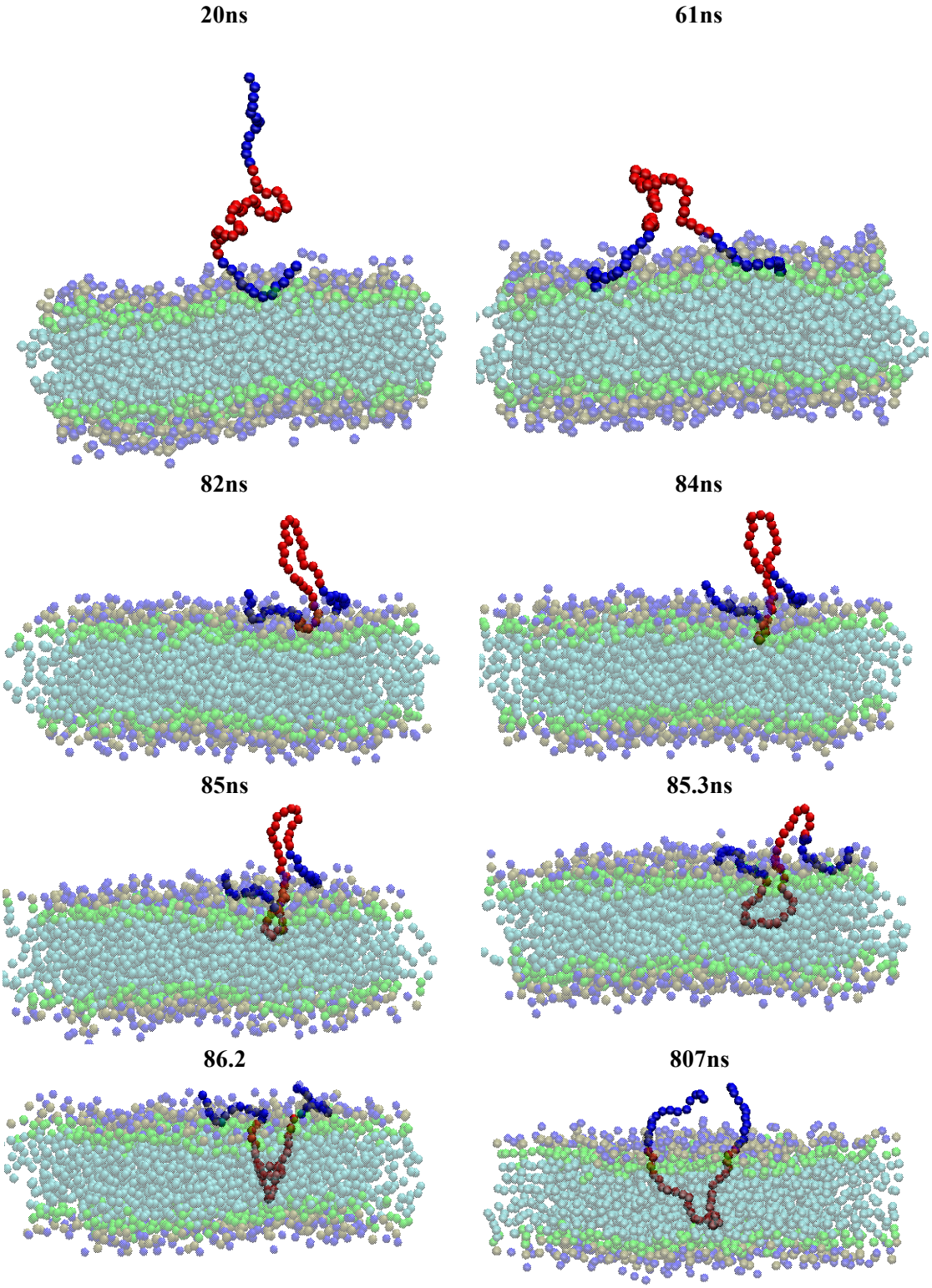

6. REFERENCES.

(1) Stubbs, J. M.; Potoff, J. J.; Siepmann, J. I. *Journal of Physical Chemistry B* **2004**, *108*, 17596.

(2) Marrink, S. J.; de Vries, A. H.; Mark, A. E. *Journal of Physical Chemistry B* **2004**, *108*, 750.

(3) Marrink, S. J.; Risselada, H. J.; Yefimov, S.; Tieleman, D. P.; de Vries, A. H. *Journal of Physical Chemistry B* **2007**, *111*, 7812.

(4) Milano, G.; Muller-Plathe, F. *Journal of Physical Chemistry B* **2005**, *109*, 18609.

(5) Hezaveh, S.; Samanta, S.; Milano, G.; Roccatano, D. *Journal of Chemical Physics* **2011**, *135*.

(6) Kawaguchi, S.; Imai, G.; Suzuki, J.; Miyahara, A.; Kitano, T. *Polymer* **1997**, *38*, 2885.

(7) Graff, A.; Benito, S. M.; Verbert, C.; Meier, W. *Polymer Nanocontainers*; Wiley-VCH Verlag GmbH & Co. KGaA, 2005.

(8) Samanta, S.; Hezaveh, S.; Milano, G.; Roccatano, D. *Journal of Physical Chemistry B* **2012**, *116*, 5141.

(9) Kumar, S.; Bouzida, D.; Swendsen, R. H.; Kollman, P. A.; Rosenberg, J. M. *Journal of Computational Chemistry* **1992**, *13*, 1011.